19. CARBON-ISOTOPE STRATIGRAPHY, SITE 577[1]

N. J. Shackleton and M. A. Hall, University of Cambridge
and
U. Bleil, Institut für Geophysik, Ruhr-Universität Bochum[2]

ABSTRACT

We have obtained a detailed carbon-isotope stratigraphy of the Paleocene sections recovered from Deep Sea Drilling Project (DSDP) Holes 577 and 577A. This ^{13}C record is useful in stratigraphically correlating the two holes and in interpreting the magnetostratigraphic data. Comparison with the published data for Site 527 (Southeast Atlantic Ocean) shows that ^{13}C stratigraphy is also valuable for long-distance correlation.

INTRODUCTION

It has been known for many years that substantial fluctuations in the level of oceanic ^{13}C occurred during the Phanerozoic. For the Cenozoic, the fluctuations were first noticed in the ^{13}C content of foraminifers (Douglas and Savin, 1971; Shackleton and Kennett, 1975). Scholle and Arthur (1980) first demonstrated important ^{13}C variations in the Mesozoic by analyzing bulk carbonate. Shackleton and Hall (1984) obtained a detailed ^{13}C stratigraphy from bulk sediment at the Leg 74 sites.

It is important to gather information on the ^{13}C stratigraphy of marine carbonates in order to understand the history of the global organic carbon budget (Scholle and Arthur, 1980; Shackleton, in press). In this context, the anomalously high ^{13}C values apparent in the late Paleocene are of particular interest because they are comparable with the ^{13}C values observed by Scholle and Arthur (1980) in association with Cretaceous ocean anoxic events. It was interest in this late Paleocene ^{13}C maximum that was the original motive for analyzing carbonates from the Paleocene section recovered at Site 577 on Leg 86.

Site 577 was cored using the hydraulic piston corer (HPC) (Site 577 chapter, this volume). The site is located on the Shatsky Rise at 32°36.51′N, 157°43.40′E in 2675 m water depth. The paleolatitude of Site 577 during the Paleocene would have been within the tropics at about 15°N, according to the reconstruction of Firstbrook, et al. (1979); paleomagnetic data for the sediments of Site 577 (Bleil, this volume) are consistent with this reconstruction. The site experienced erosion or nondeposition during most of mid-Eocene to mid-Miocene time, but the Paleocene and lower Eocene are well represented and have provided a good magnetostratigraphic record (Bleil, this volume) and a detailed nannofossil stratigraphy (Monechi, this volume; Monechi, Bleil, and Backman, this volume). The cored section consists of foraminifer–nannofossil ooze that is not lithified and was easily cored through the Cretaceous/Tertiary boundary using the HPC (Site 577 chapter, this volume); the early Paleogene section has probably never been at a significantly deeper burial depth than it is today (Schultheiss, this volume). The Cretaceous/Tertiary boundary is located at 109.6 m below the seafloor.

Methods

Samples were obtained at approximately 30-cm intervals throughout the recovered Paleocene and Eocene sections (apart from the earliest Paleocene, which is the subject of another study; Zachos et al., this volume). This sampling interval provides several samples per million years. At present, the ultimate useful resolution for ^{13}C-stratigraphic studies in bulk sediment is not known. Both Holes 577 and 577A were sampled. This was initially done in order to maximize coverage by duplicating in Hole 577A those intervals missed in Hole 577, but it subsequently became evident that the ^{13}C record is a valuable tool for determining accurate stratigraphic correlations between the two holes.

Isotope analyses were made in a VG Isogas 903 triple collector mass spectrometer using the reaction system shown in Shackleton, Hall, and Boersma (1984). Measurements are expressed with reference to the PDB (PeeDee belemnite) standard (Epstein et al., 1951) using the calibrations in Shackleton, Imbrie, and Hall (1983). The chief limitation on analytical reproducibility is that the system used is designed for small numbers of foraminifers; because of the inhomogeneity of the sediment samples it would be preferable to use larger amounts of sediment (~ 100 mg) for each analysis rather than about 1 mg, the amount used in this study. In the present study reproducibility is about ± 0.1 per mil; reproducibility at least a factor of two better is possible with homogeneous samples.

RESULTS

Carbon- and oxygen-isotope analyses are listed in Table 1. Before discussing their wider significance, it is appropriate to discuss their use in understanding the stratigraphic relationship between the two holes drilled at Site 577. The carbon- and oxygen-isotope data are plotted against reported depth below the seafloor in Figure 1. When one examines either the stable-isotope data (Fig. 1) or the biostratigraphic or magnetostratigraphic data (Monechi, Bleil, and Backman, this volume), it is readily apparent that events are not observed at precisely the same reported depth in the two holes. This discrepancy is partly the consequence of the convention by which depth is assigned to the sediment contained in an incompletely filled core barrel (Introduction and Explanatory Notes, this volume) and partly a result of uncertainty of the ex-

[1] Heath, G. R., Burckle, L. H., et al., *Init. Repts. DSDP*, 86: Washington (U.S. Govt. Printing Office).

[2] Addresses: (Shackleton and Hall) University of Cambridge, Godwin Laboratory for Quaternary Research, Free School Lane, Cambridge CB2 3RS, United Kingdom; (Bleil) Institut für Geophysik, Ruhr-Universität, 4630 Bochum, Federal Republic of Germany.

Table 1. Carbon- and oxygen-isotope data for bulk sediment carbonate from Holes 577 and 577A.

Sample (interval in cm)	Depth (m)	Adjusted depth (m)	Age (m.y.)	$\delta^{18}O$ (‰)	$\delta^{13}C$ (‰)
Hole 577					
8-4, 0-1	68.30	67.00	52.106	0.12	2.13
8-4, 30-31	68.60	67.30	52.240	0.00	2.13
8-4, 60-61	68.90	67.60	52.374	0.32	2.30
8-4, 90-91	69.20	67.90	52.508	−0.07	2.16
8-4, 120-121	69.50	68.20	52.642	−0.27	2.09
8-5, 0-1	69.80	68.50	52.775	−0.09	2.07
8-5, 30-31	70.10	68.80	52.908	−0.24	2.04
8-5, 60-61	70.40	69.10	53.040	−0.67	1.95
8-5, 90-91	70.70	69.40	53.173	−0.41	1.97
8-5, 120-121	71.00	69.70	53.306	−0.29	2.00
8-6, 0-1	71.30	70.00	53.439	−0.59	1.86
8-6, 30-31	71.60	70.30	53.571	−0.68	1.60
8-6, 60-61	71.90	70.60	53.704	−0.42	1.98
8-6, 90-91	72.20	70.90	53.837	−0.54	1.77
8-6, 120-121	72.50	71.20	53.970	−0.79	1.41
8-7, 0-1	72.80	71.50	54.103	−0.58	1.90
8,CC (17-18)	72.97	71.67	54.178	−0.35	1.71
9-1, 0-1	73.30	73.30	54.776	−0.67	1.18
9-1, 30-31	73.60	73.60	54.827	−0.58	1.53
9-1, 60-61	73.90	73.90	54.878	−0.52	1.42
9-1, 90-91	74.20	74.20	54.928	−0.46	1.20
9-1, 120-121	74.50	74.50	54.979	−0.49	1.33
9-2, 0-1	74.80	74.80	55.030	−0.45	1.39
9-2, 30-31	75.10	75.10	55.081	−0.48	1.43
9-2, 60-61	75.40	75.40	55.132	0.09	1.45
9-2, 90-91	75.70	75.70	55.183	−0.42	1.29
9-2, 120-121	76.00	76.00	55.235	−0.19	1.35
9-3, 0-1	76.30	76.30	55.287	−0.67	0.83
9-3, 30-31	76.60	76.60	55.339	−0.60	1.12
9-3, 60-61	76.90	76.90	55.391	−0.44	1.26
9-3, 90-91	77.20	77.20	55.443	−0.65	1.45
9-3, 120-121	77.50	77.50	55.495	−0.42	1.33
9-4, 0-1	77.80	77.80	55.547	−0.68	1.64
9-4, 30-31	78.10	78.10	55.599	−0.45	1.55
9-4, 60-61	78.40	78.40	55.651	−0.41	1.31
9-4, 90-91	78.70	78.70	55.740	−0.32	1.55
9-4, 120-121	79.00	79.00	55.836	−0.27	1.61
9-5, 0-1	79.30	79.30	55.932	−0.46	1.09
9-5, 30-31	79.60	79.60	56.028	−0.22	1.21
9-5, 60-61	79.90	79.90	56.124	−0.54	1.58
9-5, 90-91	80.20	80.20	56.332	−0.62	1.72
9-5, 113-114	80.43	80.43	56.509	−0.68	2.08
9-6, 0-1	80.80	80.80	56.793	−0.61	2.07
9-6, 30-31	81.10	81.10	57.024	−0.81	1.90
9-6, 60-61	81.40	81.40	57.254	−0.87	2.08
9-6, 90-91	81.70	81.70	57.485	−0.86	2.17
9-6, 120-121	82.00	82.00	57.643	−0.81	2.20
9,CC (8-9)	82.08	82.08	57.686	−0.74	2.17
10-1, 30-31	83.10	83.10	57.961	−0.76	3.28
10-1, 60-61	83.40	83.40	58.048	−0.67	3.10
10-1, 90-91	83.70	83.70	58.134	−0.81	3.22
10-1, 120-121	84.00	84.00	58.221	−0.49	3.42
10-2, 0-1	84.30	84.30	58.308	−0.75	3.24
10-2, 30-31	84.60	84.60	58.394	−0.65	3.59
10-2, 60-61	84.90	84.90	58.481	−1.08	3.53
10-2, 90-91	85.20	85.20	58.568	−0.96	3.61
10-2, 120-121	85.50	85.50	58.654	−0.94	3.45
10-3, 0-1	85.80	85.80	58.735	−0.96	3.49
10-3, 30-31	86.10	86.10	58.817	−1.03	3.07
10-3, 60-61	86.40	86.40	58.899	−0.99	3.40
10-3, 90-91	86.70	86.70	58.981	−0.93	3.79
10-3, 120-121	87.00	87.00	59.063	−0.99	3.72
10-4, 0-1	87.30	87.30	59.145	−1.13	3.66
10-4, 30-31	87.60	87.60	59.226	−1.15	3.50
10-4, 60-61	87.90	87.90	59.310	−1.13	3.52
10-4, 90-91	88.20	88.20	59.394	−1.02	3.78
10-4, 120-121	88.50	88.50	59.478	−0.92	3.80
10-5, 0-1	88.80	88.80	59.561	−1.05	3.69
10-5, 30-31	89.10	89.10	59.645	−0.85	3.85
10-5, 60-61	89.40	89.40	59.729	−1.04	3.71
10-5, 90-91	89.70	89.70	59.813	−0.86	3.76
10-5, 120-121	90.00	90.00	59.897	−0.83	3.79
10-6, 0-1	90.30	90.30	59.981	−0.78	3.90
10-6, 30-31	90.60	90.60	60.065	−0.56	3.60

Table 1. (Continued).

Sample (interval in cm)	Depth (m)	Adjusted depth (m)	Age (m.y.)	$\delta^{18}O$ (‰)	$\delta^{13}C$ (‰)
Hole 577 (Cont.)					
10-6, 60-61	90.90	90.90	60.148	−0.49	3.44
10-6, 90-91	91.20	91.20	60.232	−0.67	3.62
10-6, 120-121	91.50	91.50	60.316	−0.71	3.33
10-7, 0-1	91.80	91.80	60.400	−0.87	3.41
10-7, 30-31	92.10	92.10	60.484	−1.05	3.62
10,CC (17-18)	92.27	92.27	60.531	−1.02	3.39
11-1, 0-1	92.30	92.30	60.540	−0.96	3.82
11-1, 30-31	92.60	92.60	60.624	−0.88	3.91
11-1, 60-61	92.90	92.90	60.707	−0.87	3.65
11-1, 90-91	93.20	93.20	60.791	−0.76	3.59
11-1, 120-121	93.50	93.50	60.875	−0.62	3.55
11-2, 0-1	93.80	93.80	60.959	−0.45	3.75
11-2, 30-31	94.10	94.10	61.043	−0.47	3.29
11-2, 60-61	94.40	94.40	61.127	−1.02	3.29
11-2, 90-91	94.70	94.70	61.210	−0.37	2.78
11-2, 120-121	95.00	95.00	61.294	−0.85	3.23
11-3, 0-1	95.30	95.30	61.378	−0.54	3.18
11-3, 30-31	95.60	95.60	61.462	−0.71	3.12
11-3, 60-61	95.90	95.90	61.546	−0.86	3.04
11-3, 90-91	96.20	96.20	61.630	−0.71	2.99
11-3, 120-121	96.50	96.50	61.714	−0.58	2.98
11-4, 0-1	96.80	96.80	61.797	−0.58	3.04
11-4, 30-31	97.10	97.10	61.881	−0.88	3.08
11-4, 60-61	97.40	97.40	61.965	−0.73	2.79
11-4, 90-91	97.70	97.70	62.049	−0.62	3.05
11-4, 120-121	98.00	98.00	62.133	−0.66	2.87
11-5, 0-1	98.30	98.30	62.217	−0.46	2.91
11-5, 30-31	98.60	98.60	62.301	−0.82	2.81
11-5, 60-61	98.90	98.90	62.384	−0.59	2.89
11-5, 90-91	99.20	99.20	62.468	−0.49	2.84
11-5, 120-121	99.50	99.50	62.552	−0.55	2.59
11-6, 0-1	99.80	99.80	62.636	−0.54	2.46
11-6, 30-31	100.10	100.10	62.720	−0.40	2.59
11-6, 60-61	100.40	100.40	62.804	−0.91	2.61
11-6, 90-91	100.70	100.70	62.887	−0.81	2.70
11-6, 120-121	101.00	101.00	62.971	−0.98	2.43
11,CC (0-1)	101.30	101.30	63.090	−0.66	2.67
Hole 577A					
9-1, 4-5	75.94	75.94	55.225	−0.14	1.36
9-1, 30-31	76.20	76.20	55.272	−0.51	1.36
9-1, 60-61	76.50	76.50	55.324	−0.51	1.49
9-1, 90-91	76.80	76.80	55.374	−0.15	1.48
9-1, 120-121	77.10	77.10	55.426	−0.18	1.45
9-2, 0-1	77.40	77.40	55.478	−0.45	1.91
9-2, 30-31	77.70	77.70	55.530	−0.32	1.72
9-2, 60-61	78.00	78.00	55.582	−0.59	1.83
9-2, 90-91	78.30	78.30	55.634	−0.47	1.97
9-2, 120-121	78.60	78.60	55.708	−0.42	1.64
9-3, 0-1	78.90	78.90	55.804	−0.16	1.80
9-3, 30-31	79.20	79.20	55.900	−0.52	1.76
9-3, 60-61	79.50	79.50	55.996	−0.45	1.74
9,CC (5-6)	79.76	79.76	56.079	−0.82	1.84
10-1, 2-3	85.42	85.42	58.631	−0.92	3.58
10-1, 30-31	85.70	85.70	58.708	−0.94	3.27
10-1, 60-61	86.00	86.00	58.790	−0.96	3.57
10-1, 79-81	86.20	86.20	58.845	−0.57	3.81
10-1, 90-91	86.30	86.30	58.872	−1.12	3.69
10-1, 120-121	86.60	86.60	58.954	−0.92	3.74
10-1, 129-131	86.70	86.70	58.981	−0.88	3.74
10-2, 0-1	86.90	86.90	59.035	−0.98	3.45
10-2, 29-31	87.20	87.20	59.117	−0.84	3.77
10-2, 32-33	87.22	87.22	59.123	−0.96	3.62
10-2, 60-61	87.50	87.50	59.199	−1.06	3.33
10-2, 79-81	87.70	87.70	59.254	−1.06	3.55
10-2, 90-91	87.80	87.80	59.282	−1.06	3.51
10-2, 120-121	88.10	88.10	59.366	−0.92	3.66
10-2, 129-131	88.20	88.20	59.394	−0.96	3.88
10-3, 0-1	88.40	88.40	59.450	−0.92	3.75
10-3, 29-30	88.69	88.69	59.531	−0.76	3.86
10-3, 29-31	88.70	88.70	59.533	−1.11	3.74
10-3, 58-59	88.98	88.98	59.612	−0.88	3.83
10-3, 70-72	89.11	89.11	59.648	−1.02	3.85

Table 1. (Continued).

Sample (interval in cm)	Depth (m)	Adjusted depth (m)	Age (m.y.)	$\delta^{18}O$ (‰)	$\delta^{13}C$ (‰)
Hole 577A (Cont.)					
10-3, 90–91	89.30	89.30	59.701	−0.89	3.77
10-3, 99–101	89.40	89.40	59.729	−0.85	3.89
10-3, 120–121	89.60	89.60	59.785	−0.82	3.79
10-4, 0–1	89.90	89.90	59.869	−0.82	3.74
10-4, 28–29	90.18	90.18	59.950	−0.77	3.52
10-4, 30–32	90.21	90.21	59.956	−0.70	3.61
10-4, 60–61	90.50	90.50	60.037	−0.56	3.39
10-4, 80–82	90.71	90.71	60.095	−0.62	2.48
10-4, 90–91	90.80	90.80	60.120	−0.56	3.52
10-4, 118–119	91.08	91.08	60.199	−0.56	3.39
10-4, 129–131	91.20	91.20	60.232	−0.39	3.58
10-5, 0–1	91.40	91.40	60.288	−0.93	3.50
10-5, 30–31	91.70	91.70	60.372	−0.96	3.40
10-5, 31–33	91.72	91.72	60.378	−1.02	3.38
10-5, 60–61	92.00	92.00	60.456	−0.96	3.48
10-5, 80–82	92.21	94.85	61.252	−0.92	3.49
10-5, 90–91	92.30	94.92	61.272	−0.84	3.52
10-5, 120–121	92.60	95.14	61.333	−0.84	3.36
10-5, 129–131	92.70	95.21	61.353	−0.79	3.20
10-6, 0–1	92.90	95.35	61.392	−0.71	3.11
10-6, 30–31	93.20	95.57	61.454	−0.65	3.02
10-6, 34–46	93.25	95.61	61.465	−0.80	3.03
10-6, 60–61	93.50	95.79	61.515	−0.76	3.12
11-1, 0–1	94.90	96.81	61.800	−0.61	2.88
11-1, 30–31	95.20	97.03	61.862	−0.68	2.74
11-1, 60–61	95.50	97.25	61.920	−0.70	2.75
11-1, 90–91	95.80	97.46	61.982	−0.54	2.85
11-1, 120–121	96.10	97.68	62.041	−0.58	2.81
11-2, 0–1	96.40	97.90	62.105	−0.52	2.81
11-2, 30–31	96.70	98.12	62.166	−0.32	2.78
11-2, 60–61	97.00	98.34	62.225	−0.50	2.43
11-2, 90–91	97.30	98.55	62.287	−0.60	2.34
11-2, 120–121	97.59	98.76	62.345	−0.75	2.63
11-3, 0–1	97.90	98.99	62.410	−0.77	2.64
11-3, 30–31	98.20	99.21	62.471	−0.61	2.53
11-3, 60–61	98.49	99.42	62.530	−0.72	2.48
11-3, 90–91	98.80	99.64	62.591	−0.77	2.32
11-3, 120–121	99.10	99.86	62.653	−0.62	2.36
11-4, 0–1	99.40	100.08	62.714	−0.80	2.16
11-4, 30–31	99.70	100.30	62.776	−0.58	2.45
11-4, 60–61	100.00	100.51	62.834	−0.86	2.43
11-4, 90–91	100.30	100.73	62.896	−0.64	2.42
11-4, 120–121	100.60	100.95	62.957	−0.85	2.31
11-5, 0–1	100.90	101.17	63.019	−0.64	1.97
11-5, 30–31	101.20	101.39	63.136	−0.67	2.54
11-5, 60–61	101.50	101.61	63.288	−0.77	2.52
11-5, 90–91	101.80	101.82	63.434	−1.03	2.36
11-5, 120–121	102.10	102.10	63.607	−0.69	2.38
11-6, 0–1	102.40	102.40	63.773	−0.83	2.20
11-6, 30–31	102.70	102.70	63.940	−0.87	2.33
11-6, 60–61	103.00	103.00	64.101	−0.89	1.91
11-6, 90–91	103.30	103.30	64.273	−0.74	1.98
11-6, 120–121	103.60	103.60	64.396	−1.09	2.13
11-7, 0–1	103.90	103.90	64.513	−0.96	1.96
11,CC (5–6)	104.15	104.15	64.603	−1.00	2.08

Note: Both reported depth below sea level and depth as adjusted according to Table 2 are given (see text). Note that "reported depth" is consistent with DSDP records and should be used to collate these data with those contained in other chapters in this volume. Ages are also given as estimated by linear interpolation between the control points in Table 3.

act depth of the corer below the seafloor at the moment of deployment. Until the advent of the HPC, little consideration was given to the problems involved in making a precise stratigraphic correlation between two adjacent holes other than in terms of reported depth below seafloor. It is now becoming important to do this, especially in order to obtain accurate accumulation-rate data, as attempted by Shackleton and Members of the Shipboard Scientific Party (1984).

Both carbonate content (within a limited geographical area; e.g., Arrhenius, 1952; Crowley, 1981) and oxygen-isotope stratigraphy (globally; e.g., CLIMAP, 1976; Shackleton, 1977) have been used for many years to correlate accurately Pleistocene deep-sea records. Varying carbonate content provides a good signal only if carbonate content is well below 100%, and conventional isotope stratigraphy is labor intensive because much time is spent picking the appropriate species for analysis. In any case, the use of oxygen-isotope variations for stratigraphic correlation is dependent on substantial ocean-isotope variations resulting from ice-volume variations and hence would not apply in the Paleocene. Carbon-isotope stratigraphy in bulk sediment can be performed more rapidly because less time is required to prepare the samples; for this reason it is interesting to explore its potential for use in correlation studies.

In the case of Site 577, when the ^{13}C data for the two holes were plotted using the paleomagnetic stratigraphy as it was first interpreted, it became apparent that an inconsistency had arisen. The two measurements of normal polarity that were originally interpreted as representing Chron C-26N in Hole 577 (Samples 577-10-6, 141 cm and 577-10-7, 10 cm; 91.72 to 91.91 m sub-bottom) and the two that were interpreted as representing Chron C-26N in Hole 577A (Samples 577A-10-3, 70 cm and 577A-10-3, 91 cm; 89.11 to 89.40 m sub-bottom) fall at different points in the ^{13}C record. Moreover, these events occur in sediments with significantly different ^{13}C contents. An additional normally magnetized interval was found in Hole 577 (Sample 577-10-5, 89 cm; 89.70 m sub-bottom); since this was observed only in a single sample it would usually be ignored by a conservative magnetostratigrapher. However, the ^{13}C stratigraphy suggests that it is this event, and not the deeper normal event in Hole 577 (Samples 577-10-6, 141 cm and 577-10-7, 10 cm; 91.72 to 91.91 m sub-bottom), that is precisely correlated with the normal event recorded in Hole 577A (Samples 577A-10-3, 70 cm and 577A-10-3, 91 cm; 89.11 to 89.40 m sub-bottom).

Inspection of the ^{13}C data shown in Figure 1 indicates that the peak of isotopically heavy values in the top of Core 577-11 between 92.3 and 93.8 m sub-bottom is not present in Hole 577A. The detailed biostratigraphic studies of Monechi, Bleil, and Backman (this volume) suggest that, if the reason is that some sediment is missing in Hole 577A, the sediment must be missing from just above the base of Core 577A-10, because the detailed biostratigraphic analysis of Site 577 shows that the missing section is above the *Heliolithus kleinpellii* peak that is present at the bottom of Core 577A-10. Close inspection of the two ^{13}C records leads us to the same conclusion. We have therefore attempted to estimate the position below the seafloor at which the sediment in each core barrel most probably lay (assuming that the strata were horizontal between the two holes), using only features in the ^{13}C record and magnetic reversals to estimate the offsets.

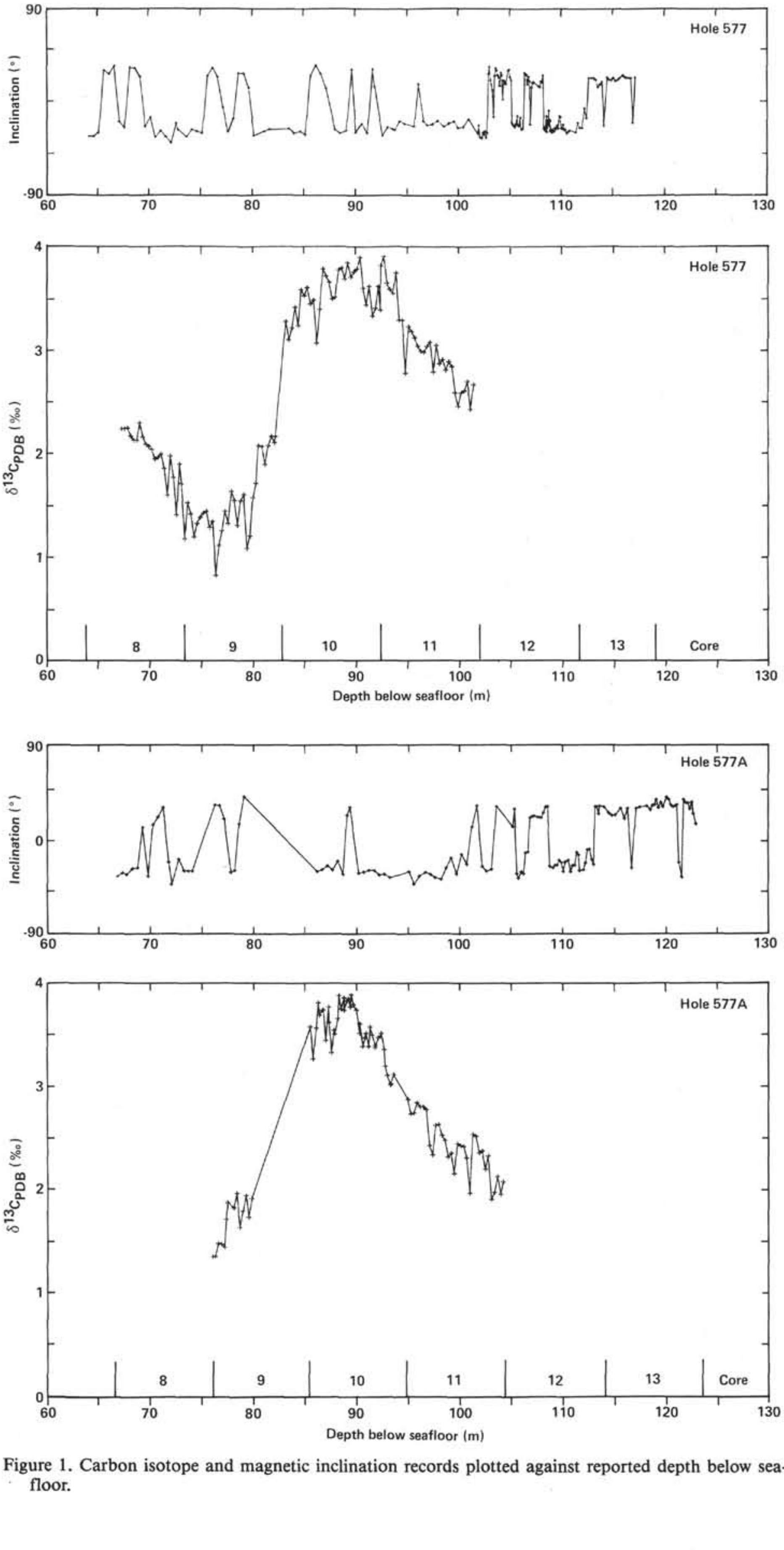

Figure 1. Carbon isotope and magnetic inclination records plotted against reported depth below seafloor.

Table 2 gives the adjusted sub-bottom depth figures assigned. In order to minimize the amount of distortion of reported depths, we have assumed that the chief problem is a stretching of Core 577A-11. We have therefore made a downward adjustment of the top of Core 577A-11, as well as a small section of Core 10, while holding the base of Core 11 fixed. Aside from this distortion, the same depth adjustment is applied to the top and bottom of each sediment core recovered.

In Table 1, each sample is assigned two depths: that used in DSDP records and a second depth that represents our estimate of the most likely depth at which the sample actually lay below the seafloor (using the adjustments in Table 2). Since most of the cores in Hole 577 had a high recovery, it is the Hole 577A cores that are more likely to require adjustment; however, one has to consider the continuity of the whole column when making such adjustments. For this reason, the discrepancy has been distributed equally between Core 577-8 and Core 577A-8. As will be seen, comparison with the ^{13}C data from Site 527 suggests that the Hole 577 record at this point is correct and that there is indeed a section of over 1.5 m thickness missing in Core 577A-10.

The adjusted carbon-isotope data are plotted against estimated age in Figures 2 and 3 by assigning ages (Berggren et al., in press) to the magnetic boundaries at their newly assigned depths, as shown in Table 3. In view of potential uncertainty as to the identification of Chron C-26N, the sections were interpolated over the interval between Chrons C-25N to C-27N. Using this procedure, the normal event that (according to the ^{13}C stratigraphy) is common to both sites has an interpolated age of about 59.7 m.y.; in Hole 577 two additional magnetically normal events were observed with interpolated ages of about 60.4 and 61.7 m.y. For convenience, the magnetic data are replotted in Figures 2 and 3 according to this age model.

Table 2. Control points for converting reported depths to adjusted depths for the purpose of reporting data from both holes on a common depth scale (m).

Hole 577			Hole 577A		
Control point	Depth Reported	Depth Adjusted	Control point	Depth Reported	Depth Adjusted
Core 8			Core 8		
Top	63.8	62.5	Top	66.4	67.7
Base	73.29	71.99	8-5, 140 cm	73.8	75.1
Core 9			Core 9		
Top	73.3	73.3	Top	75.9	75.9
Core 11			Base	85.4	85.4
Base	101.59	101.59	Core 10		
Core 12			Top	85.4	85.4
Top	101.6	101.95	10-5, 60 cm	92.0	92.0
Core 13			10-5, 62 cm	92.02	94.72
Base	118.8	119.15	Core 11		
			11-5, 100 cm	101.9	101.9
			Base	104.4	104.4
			Core 12		
			Top	104.4	104.4
			Core 13		
			Base	123.4	123.4

Note: In Hole 577A we have assumed that there was some loss of sediment at about Sample 577A-10-5, 60 cm and that there was some stretching in Core 11; the model we have used compresses the recovered sediment linearly between 92.02 m and 101.9 m.

Although it has no bearing on the present discussion, it should be noted that the lowest control point has been taken at the first appearance of *Micula mura* since the proximity of this datum to the samples interpreted as correlative with the base of Chron C-30N appears to be inconsistent with the age estimate in Shackleton et al. (1984), suggesting the possibility of a hiatus at this point. Before we can use Site 577 material to estimate tropical productivity in the Late Cretaceous, the viability of this interpretation of the Maestrichtian record, as opposed to the more inherently likely one proposed by Bleil (this volume), must be investigated further.

DISCUSSION

The preceding data suggest that the identification of Chron C-26N may prove more difficult than expected. According to the time scale of Berggren et al. (in press), Chron C-26N had a duration of 0.54 m.y. (60.75–60.21 m.y. ago). The normal event at an interpolated age of 59.7 m.y.) is bounded above and below by reversed samples (in both holes) and has an estimated duration of less than 0.5 m.y. (Hole 577, one sample) and between 0.1 and 0.5 m.y. (Hole 577A, two samples). The normal event at the interpolated age of 60.4 m.y. in Hole 577 is at the bottom of a core and can only be assigned a minimum duration of about 0.2 m.y. (2 samples); the oldest unidentified normal event can again only be assigned a duration of less than 0.5 m.y., being represented by only a single normally magnetized sample.

Which of these three normal events should be correlated with Chron C-26N cannot be decided definitively merely by stating that the middle of the three best fits the assigned for Chron C-26N, since there is no particular reason to believe that the sediment accumulated at a uniform rate. The marine magnetic anomaly sequence should perhaps be reinspected for evidence of more than one normal event in this interval. If there was not, in fact, a single normal event with a duration as long as is usually assigned to Anomaly 26, this would explain why some sites have not detected a normal event between Chrons C-25N and C-27N (Berggren et al., in press, table 4) although the marine magnetic records suggest that Anomaly 26 is a clear entity (Dan Mackenzie, pers. comm., 1984).

It is uncertain whether any of the three normal events just mentioned should be correlated with the one found in Sites 527 and 529 and interpreted there as C-26N (Shackleton et al., 1984). Figure 4 shows the ^{13}C bulk sediment record of Site 527 plotted using the age control points of Shackleton et al. (1984, table 1). Although the reliability of long-distance ^{13}C correlations has not been established, comparison of Figures 2 and 4 suggests that this may prove to be a valuable tool. The position of the magnetically normal event in Site 527 (which was assumed to represent the base of Chron C-26 for the purpose of constructing Fig. 4) in the ^{13}C record suggests that it is not correlative with any of the three magnetic normal events in Hole 577. It may be noticed that there are oth-

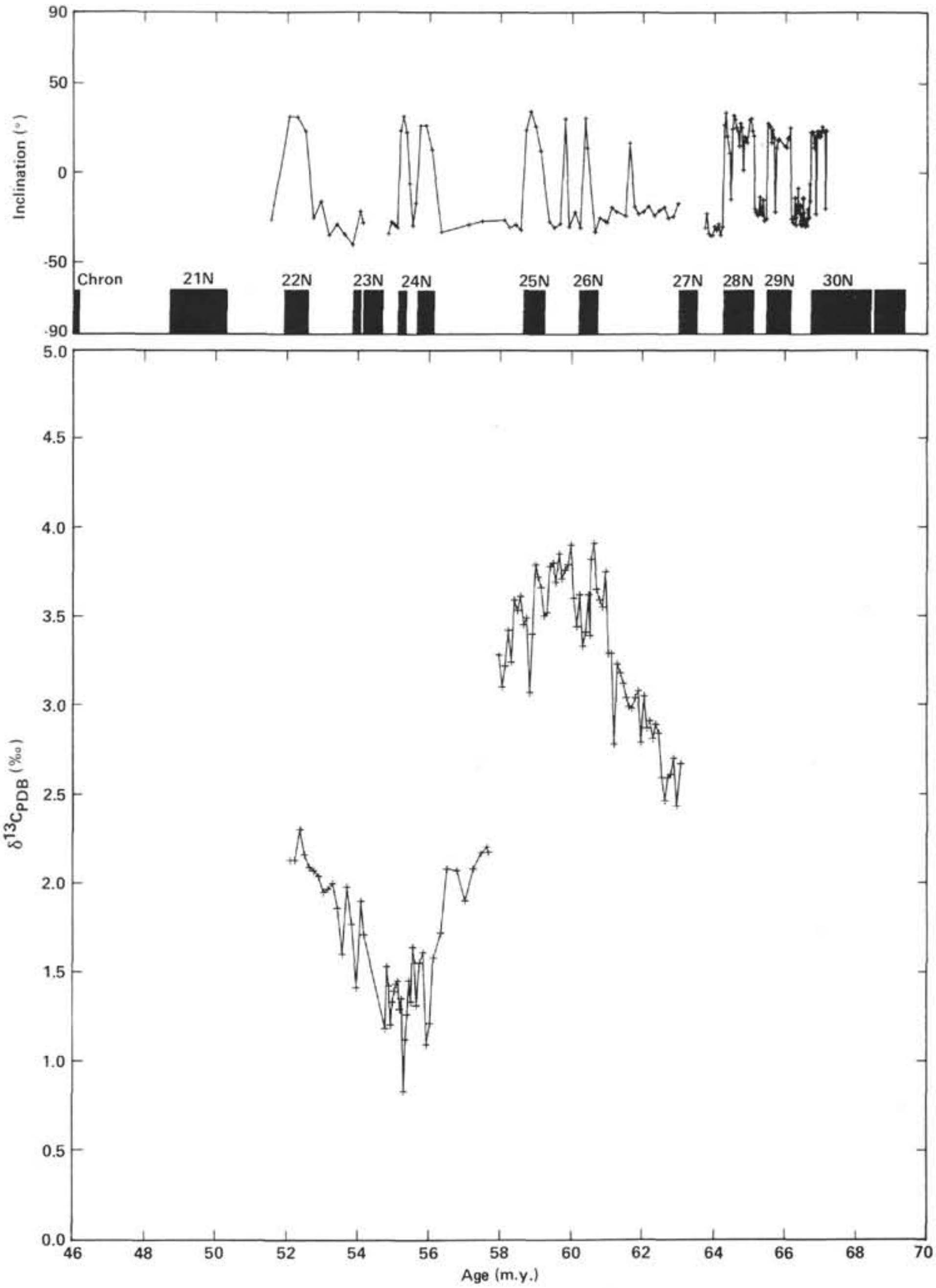

Figure 2. Magnetic record (above) and carbon-isotope record (below) of Hole 577 plotted on a time scale using linear interpolation between the control points in Table 3. The marine magnetic anomaly time scale of Berggren et al. (in press) that was used to create the time scale is shown in the center.

er sections in which three normal events have been recognized in the region of C-26N: the Contessa Highway Section (Lowrie et al., 1982), Site 524 (Tauxe et al., 1984) and the Pietralata Section (Alvarez and Lowrie, 1984).

Comparison of Figures 2 and 3 with Figure 4 shows not only that two sites in different oceans and water masses show similar features in their ^{13}C records, but that the absolute ^{13}C values are also remarkably similar. This implies that a global bulk sediment ^{13}C record should be available on the basis of data from only a few sites. Only further work will reveal whether the subtle differences between the records of Sites 577 and 527 should be interpreted as implying gaps in one or the other record, or as an indication of the limits of detailed ^{13}C correlation.

The cause of the ^{13}C peak during the Paleocene is not known. The unusually high ^{13}C values may be explained as a compensation for the global extinctions and drop in productivity at the Cretaceous/Tertiary boundary, which must have led to an imbalance in the effectiveness with which nutrients in the oceans were utilized. There may have been a buildup in oceanic nutrient levels so that the subsequent increase in diversity a few million years into the Tertiary may have led to the recolonization of an ocean that was anomalously rich in nutrients, permitting an in-

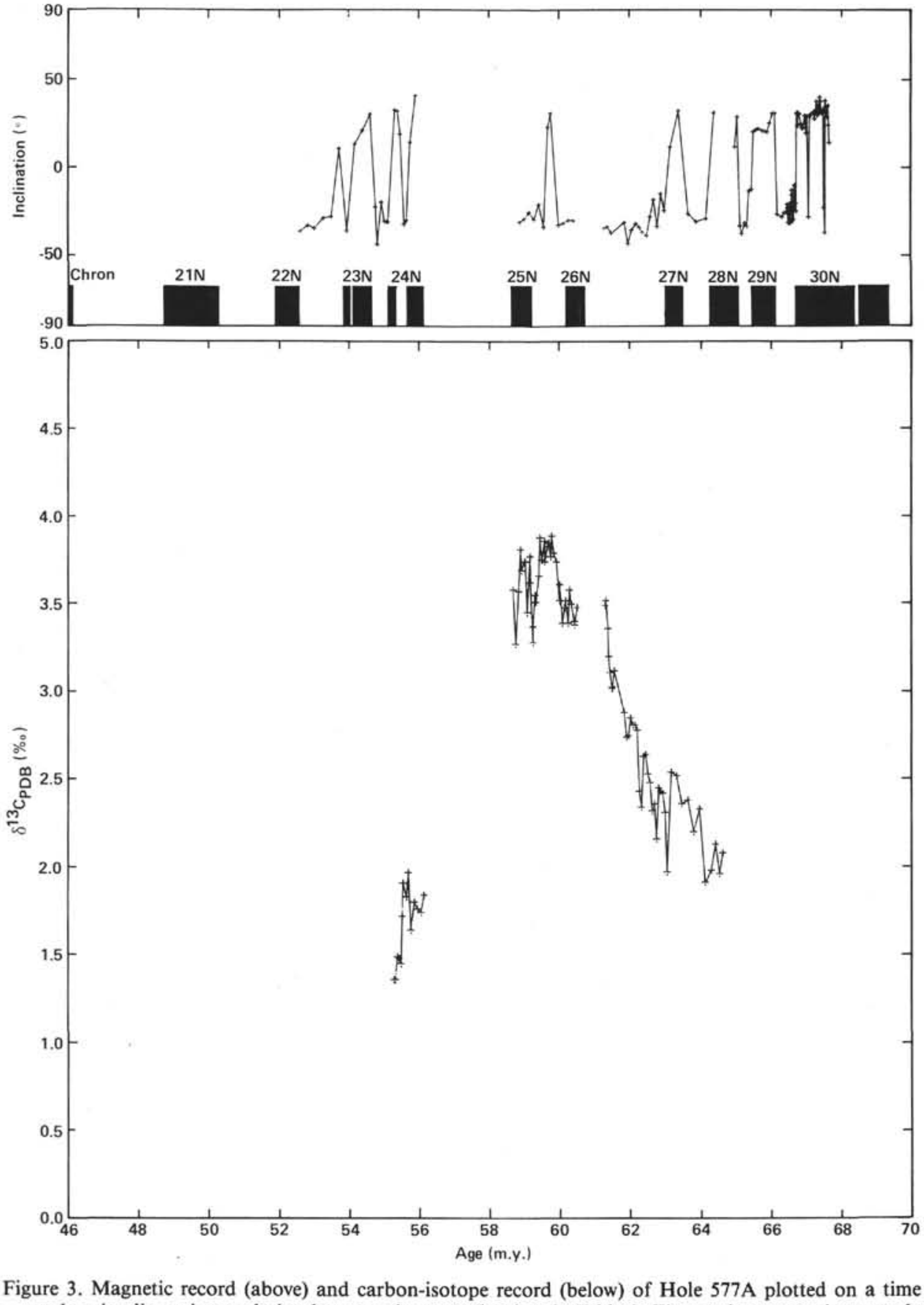

Figure 3. Magnetic record (above) and carbon-isotope record (below) of Hole 577A plotted on a time scale using linear interpolation between the control points in Table 3. The marine magnetic anomaly time scale of Berggren et al. (in press) that was used to create the time scale is shown in the center.

creased burial rate for organic matter. There is certainly scope for developing a model along these lines. However, the drop in ^{13}C very close to the top of the Paleocene is not predicted by such a model; this seems to imply an even more dramatic crash in marine productivity than at the Cretaceous/Tertiary boundary, whereas in reality the end of the Paleocene was probably a time of relatively modest faunal turnover.

CONCLUSIONS

Carbon-isotope measurements in bulk sediment from Holes 577 and 577A have been useful in aiding detailed correlation between these two holes. A very close similarity between the ^{13}C record of Site 577 and that of Site 527 (South Atlantic) suggests that the ^{13}C history of global oceanic carbonate can be quite well characterized by a single ^{13}C record. Moreover the development of a standard ^{13}C record for the Cenozoic will be of considerable value in elucidating the stratigraphy of individual sites, perhaps to a better resolution than that afforded by biostratigraphic methods.

ACKNOWLEDGMENTS

Isotope analysis in Cambridge is supported by NERC grant GR3/3606. We are grateful to Jan Backman for helpful discussion on these sediments, and to Richard Corfield, Jan Backman, Michael Arthur,

Table 3. Control points for conversion of adjusted depths to ages using magnetostratigraphic time scale of Berggren et al. (in press).

Adjusted depth (m)	Assigned age (m.y.)	Identification
64.15	48.75	Top Chron C-21N
65.65	50.34	Base Chron C-21N
66.65	51.95	Top Chron C-22N
68.15	52.62	Base Chron C-22N
72.85	54.7	Base Chron C-23N
75.45	55.14	Top Chron C-24N-2
78.45	55.66	Top Chron C-24N-1
79.95	56.14	Base Chron C-24N-1
82.6	57.8	^{13}C change
85.45	58.64	Top Chron C-25N
87.65	59.24	Base Chron C-25N
101.21	63.03	Top Chron C-27N
101.98	63.54	Base Chron C-27N
103.33	64.29	Top Chron C-28N
105.53	65.12	Base Chron C-28N
106.78	65.50	Top Chron C-29N
108.68	66.17	Base Chron C-29N
109.4	66.46	Cretaceous/Tertiary boundary
113.02	66.74	Top Chron C-30N
121.0	67.5	Base *Micula mura*

Note: Control points for the Cretaceous/Tertiary boundary and the first appearance of *Micula mura* as estimated by Shackleton et al. (1984) have been inserted to facilitate future comparison with the older part of the records from DSDP Leg 74. Also, an age of 57.8 m.y. has been assigned to the midpoint of the major ^{13}C change.

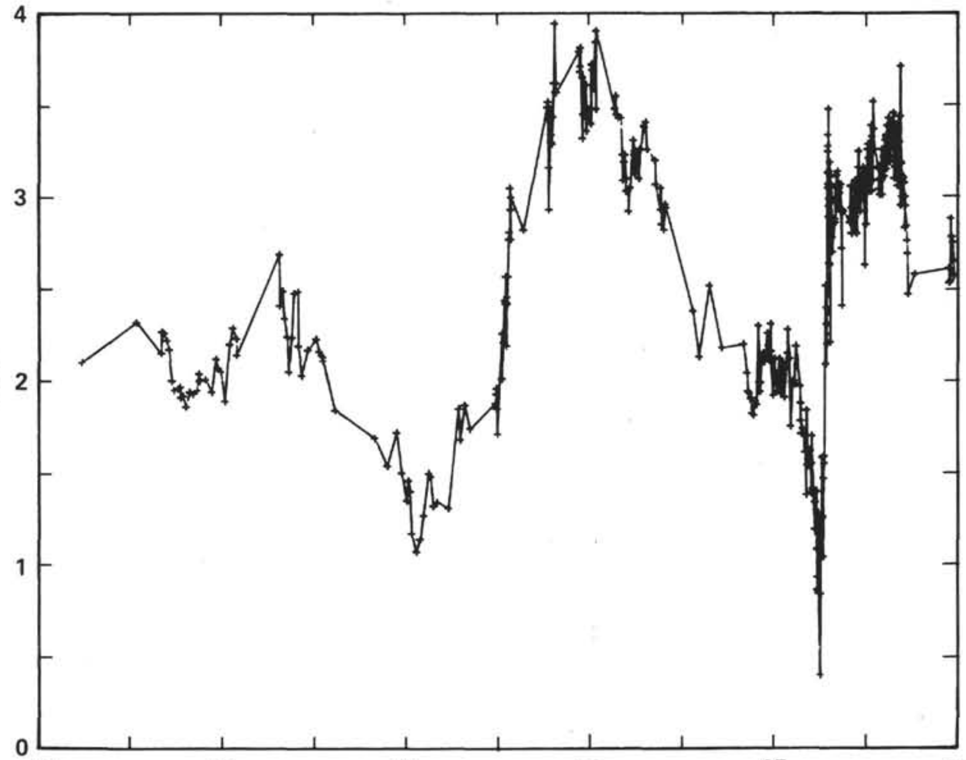

Figure 4. Carbon-isotope record of Site 527 (Shackleton and Hall, 1984, and additional unpublished measurements) using the time scale of Shackleton et al. (1984).

Peter Scholle, and Audrey Wright for reviewing an earlier draft of the manuscript.

REFERENCES

Alvarez, W., and Lowrie, W., 1984. Magnetic stratigraphy applied to synsedimentary slumps, turbidites, and basin analysis: the Scaglia Limestone at Furlo (Italy). *Geol. Soc. Am. Bull.*, 95:324–336.

Arrhenius, G., 1952. Sediment cores from the East Pacific. *Swedish Deep-Sea Exped. Repts.*, 5:6–227

Berggren, W. A., Kent, D. V., and Flynn, J. J., in press. Paleogene geochronology and chronostratigraphy. *In* Snelling, N. J. (Eds.), *Geochronology and the Geological Record*. Spec. Publ. Geol. Soc. London.

CLIMAP project members, 1976. The surface of the ice-age earth. *Science*, 191:1131–1137.

Crowley, T. J., 1981. Temperature and circulation changes in the eastern North Atlantic during the last 150,000 years: evidence from the planktonic foraminiferal record. *Mar. Micropaleontol.*, 6:97–129.

Douglas, R. G., and Savin, S. M., 1971. Isotopic analyses of planktonic foraminifera from the Cenozoic of the Northwest Pacific, Leg 6. *In* Fischer, A. G., Heezen, B. C., et al., *Init. Repts. DSDP*, 6: Washington (U.S. Govt. Printing Office), 1123–1130.

Epstein, S. M., Buchsbaum, R., Lowenstam, H. A., and Urey, H. C., 1951. Carbonate-water isotopic temperature scale. *Geol. Soc. Am. Bull.*, 62:417–426.

Firstbrook, P. L., Funnell, B. M., Hurley, A. M., and Smith, A. G., 1979. *Paleoceanic Reconstructions 160–0 Ma*: La Jolla, California (Deep Sea Drilling Project).

Lowrie, W., Alvarez, W., Napoleone, G., Perch-Nielsen, K., Premoli Silva, I., and Toumarkine, M., 1982. Paleogene magnetic stratigraphy in Umbrian pelagic carbonate rocks: the Contessa sections, Gubbio. *Geol. Soc. Am. Bull.*, 93:414–432.

Scholle, P. A., and Arthur, M., 1980. Carbon isotope fluctuations in Cretaceous pelagic limestones: potential stratigraphic and petroleum exploration tool. *Am. Assoc. Pet. Geol. Bull.*, 64:67–87.

Shackleton, N. J., 1977. The oxygen isotope stratigraphic record of the Late Pleistocene. *Philos. Trans. R. Soc. London Ser.* B,280: 169–179.

________, in press. The carbon isotope record of the Cenozoic. *In* Brooks, J., and Fleet, A. J. (Eds.), *Petroleum Source Rocks*: Oxford (Blackwells).

Shackleton, N. J., and Hall, M. A., 1984. Carbon isotope data from Leg 74 sediments. *In* Moore, T. C., Jr., Rabinowitz, P. D., et al., *Init. Repts. DSDP*, 74: Washington (U.S. Govt. Printing Office), 613–619.

Shackleton, N. J., Hall M. A., and Boersma, A., 1984. Oxygen and carbon isotope data from Leg 74 foraminifers. *In* Moore, T. C., Jr., Rabinowitz, et al., *Init. Repts. DSDP*, 74: Washington (U.S. Govt. Printing Office), 599–612.

Shackleton, N. J., Imbrie, J., and Hall, M. A., 1983. Oxygen and carbon isotope record of East Pacific core V19-30: implications for the formation of deep water in the late Pleistocene North Atlantic. *Earth Planet. Sci. Lett.*, 65:233–244.

Shackleton, N. J., and Kennett, J. P., 1975. Paleotemperature history of the Cenozoic and the initiation of Antarctic glaciation: oxygen and carbon isotope analyses in DSDP Sites 277, 279, and 281. *In* Kennett, J. P., Houtz, R. E., et al., *Init. Repts. DSDP*, 29: Washington (U.S. Govt. Printing Office), 743–756.

Shackleton, N. J., and Shipboard Scientific Party, 1984. Accumulation rates in Leg 74 sediments. *In* Moore, T. C., Jr., Rabinowitz, P. D., et al., *Init. Repts. DSDP*, 74: Washington (U.S. Govt. Printing Office), 621–644.

Tauxe, L., Tucker, P., Petersen, N. P., and LaBrecque, J. L., 1984. Magnetostratigraphy of Leg 73 sediments. *In* Hsü, K. J., LaBrecque, J. L., et al., *Init. Repts. DSDP*, 73: Washington (U.S. Govt. Printing Office), 609–621.

Date of Initial Receipt: 29 February 1984
Date of Acceptance: 6 August 1984